ISSN 1061-9348, Journal of Analytical Chemistry, 2017, Vol. 72, No. 13, pp. 1331–1339. © Pleiades Publishing, Ltd., 2017.
Original Russian Text © I.V. Sulimenkov, V.S. Brusov, V.V. Zelenov, M.G. Skoblin, V.V. Filatov, A.R. Pikhtelev, V.I. Kozlovskii, 2016, published in Mass-spektrometriya, 2016, Vol. 13, No. 4, pp. 258–267.

ARTICLES

Study of Gaseous Sample Ionization by Excited Particles Formed in Glow Discharge Using High-Resolution Orthogonal Acceleration Time-of-Flight Mass Spectrometer

I. V. Sulimenkov[a], V. S. Brusov[a], V. V. Zelenov[a], M. G. Skoblin[a], V. V. Filatov[a], A. R. Pikhtelev[a], and V. I. Kozlovskii[a, b, *]

[a] *Institute for Energy Problems of Chemical Physics, Chernogolovka, Moscow oblast, 142432 Russia*
[b] *Institute of Physiologically Active Compounds, Russian Academy of Sciences, Chernogolovka, Moscow oblast, 142432 Russia*
**e-mail: v.i.kozlovskiy@gmail.com*

Received December 15, 2015; in final form, August 31, 2016

Abstract—The experimental results of a mass spectral analysis of volatile organic compounds in a gaseous sample, obtained using an original design of an ion source based on the Penning ionization of a gas sample by excited metastable inert gas atoms, are presented. Using ANSYS software, a gas-dynamic simulation of reagent gas flow from discharge zone to ionization region was carried out to analyze the effect of gas flow profile on the transport of metastable atoms and ionization efficiency. The *n*-octane and toluene samples diluted with helium at 100 ppb mole concentrations were used for our experiments. The resulting mass spectra of *n*-octane and toluene samples containe far more intensive molecular ions in comparison to *n*-octane and toluene electron ionization mass spectra from the NIST database. The sensitivity of 5 ions per 1 pg and 130 ions per 1 pg was achieved for *n*-octane and toluene molecular ions using the developed ion source combined with our mass spectrometer. The corresponding detection limits are 2.3 pg s^{-1} for *n*-octane molecular ions and 0.08 pg s^{-1} for toluene molecular ions. The detection limit for the reported ion source was considered theoretically.

Keywords: time-of-flight mass spectrometry, ion source, glow discharge, Penning ionization, radio frequency quadrupole, detection efficiency, quantitative analysis

DOI: 10.1134/S1061934817130111

INTRODUCTION

Electron ionization is conventionally used for the mass spectrometric analysis of volatile nonpolar compounds [1]. This method is universal, as the efficiency of ionization at electron energies significantly exceeding the ionization threshold is almost independent of the class of compounds. However, there are many organic compounds providing no signals of molecular ions and deprotonated molecules in their electron ionization mass spectra. Therefore, an approach using databases was developed to identify compounds by electron ionization mass spectra. This approach is quite effective; however, if there is a mixture of compounds from one class, for example, hydrocarbons, the same fragment ions can be fragments of different initial molecular ions. Therefore, for the reliable identification of compounds, it is important to have intense molecular ion peaks in the mass spectrum. An ion source was created in [2], in which the analyte contained in a supersonic helium flow was ionized ("cold" ionization by electrons). This approach enables an increase in the fraction of molecular ions of the analyte in the electron ionization spectrum. Using the method of chemical ionization [3–5] enables one to obtain intense peaks of molecular ions for a variety of compounds. This method is sensitive, although it differs in selectivity with respect to different classes of compounds, which requires the selection of reagent ions. The efficiency of chemical ionization depends on the ion–molecular reactions rate; therefore, it is necessary to use a high concentration of reagent ions. This tightens the requirements for the operating mode of the ion source, where the reagent ions are formed by means of electron ionization at an increased pressure of the reagent gas. At present, atmospheric pressure chemical ionization methods (atmospheric pressure chemical ionization (**APCI**), direct analysis in real time (**DART**), atmospheric pressure glow discharge (**APGD**), and selected-ion flow-tube (**SIFT**) mass spectrometry) are also used, which yield stable molecular ions and protonated or deprotonated molecules of the analyte. The efficiency of the analysis in these methods is also related to the transport of sample ions from the atmospheric pressure region to mass analyzer. Ion losses arise during transportation through the differential pumping stages and as a result of unde-

sirable ion–molecular reactions with impurities in the buffer gas. The effect of such undesirable reactions is enhanced by the considerable time of ion transport from the atmospheric pressure region to the vacuum.

It is known that many atomic gases have excited metastable states with excitation energies exceeding the ionization threshoulds of many organic molecules. Such metastable atoms of inert gases are formed in high concentrations in a glow discharge. In 1963, a chromatographic detector was proposed where ionization of a sample occurred under the action of metastable inert gas atoms [6]. This method showed high detection limit for trace amounts of alkanes (at the level of 10^{-11} mol s^{-1}). Later, ion sources with a glow discharge were developed and used for mass spectrometric detection of gas samples [7–9]. A glow discharge is also used for mass spectrometric analysis of the composition of solid samples [10, 11]. When a gas sample is introduced into the low-pressure glow discharge region, the mass spectrum of the analyte ions formed is similar to the electron ionization mass spectrum, because electrons and ions in a glow discharge are accelerated in a constant or alternating electric field that supports the glow discharge. That is why to exclude the effect of high-energy ions and electrons, the ion source design was proposed where the gas flow from the discharge at a pressure of several kilopascals was mixed with the gas sample flow, and then the combined flow with the formed ions was directed to a quadrupole mass analyzer [12]. When the sample is ionized with a glow discharge at atmospheric pressure, the mass spectrum contains intense peaks of molecular ions and deprotonated sample molecules and markedly less intense peaks of fragment ions [13]. However, the transport of ions from the atmospheric pressure region to the vacuum region is associated with large losses in the differential pumping stages of interface. The construction of an ion source with the ionization of a gas sample by a pulsed glow discharge was proposed [14], where an orthogonal acceleration time-of-flight mass spectrometer (**OA–TOF–MS**) was used to record sample ions under controlled delay between the discharge pulse and the ion extraction pulse of the mass analyzer. In this way, it was possible to control the relationship between the intensity of the molecular ion peak in the mass spectrum and the intensities of the fragment ion peaks. Recently, the configuration of an ion source using active particles from a glow discharge to ionize organic compounds in gas samples has been patented [15], where a "conditioner" was used to cut off a penetration of electrons from the glow discharge zone to the ionization region. The same authors demonstrated a number of mass spectra of organic compounds obtained using an ion source of this type;the molecular ion peaks in the spectra are maximal or even the only ones [16]. According to [16], the sensitivity for hexachlorobenzene is ~800 rel. units pg^{-1}. The glow discharge is also used to analyze gas samples in IONICON mass spectrometers [17]. In such an implementation of an ion source with a glow discharge, the ionization region is a drift tube operating at a pressure of several hundreeds Pa. In this case the sample molecules can be ionized both by exchange mechanism, when the sample is ionized in collisions with H_3O^+ reagent ions formed in the glow discharge and by the Penning mechanism involving metastable krypton atoms that have an excitation energy close to the ionization energy of organic molecules. The sensitivity in the above system is 200 counts for trichlorobenzene per 1 ppbv with a sample flow rate of 25 cm^3 min^{-1}, which according to our estimates is ~60 counts pg^{-1}.

As already mentioned, one of the properties of a glow discharge is a high concentration of excited metastable gas atoms in the discharge zone, with an excitation energy sufficient for the ionization of most organic molecules. It is known from a number of works on the experimental measurement and theoretical simulation of processes in a glow discharge that the maximum concentration of excited argon atoms in the discharge is ~10^9 to 10^{11} cm^{-3} at a pressure in the discharge zone in the range of 100–10^5 Pa [18, 19]. These particles are neutral; they move with the gas flow from the glow discharge and do not "feel" in their path permanent and alternating electric fields. This feature was decided to be used in the proposed design of the ion source [20–23]. In order to increase the transport efficiency of the sample ions to the next stage of the OA–TOF–MS interface with a pressure of 0.1–1 Pa, the focusing radio-frequency (**RF**) quadrupole field was formed in ionization region where the sample molecules interact with the active particles from the glow discharge.

EXPERIMENTAL

The ion source with ionization of gas sample by active particles from glow discharge was used in combination with high-resolution OA–TOF–MS [24]. Block diagram of the experimental setup is shown in Fig. 1. Note that the interface design uses the so-called "passive pumping" of a large RF quadrupole: the same turbomolecular pump is used to evacuate the region of DC ion optics and the large RF quadrupole. At the same time, one turbomolecular pump is "saved," but the size of the skimmer opening through which the ions from the ion source enter the large RF quadrupole is limited; accordingly, the sensitivity of the mass spectrometric system is limited.

An ion source based on an electrodeless capacitive glow discharge was used to ionize the gas sample [21]. The glow discharge zone and the ionization region are separated in space. The glow discharge is organized inside a glass tube 20 cm in length and 4.5 mm in inner diameter. It is possible to change the flow rate of the reagent gas by means of MKS Baratron control unit (variation of the gas flow rate from 0 to 1000 cm^3 min^{-1}).

Small RF quadrupole is located at a distance of 5 mm from the output end of the glass tube; the quadrupole rod diameter is 5 mm, rod length is 5 cm, and the inscribed quadrupole radius is 5 mm. It was shown earlier that a quadrupole of such dimensions effectively focuses ions in the range of buffer gas pressures from 10 to 700 Pa [25–27]. The gas sample to be studied is injected into a gas flow with active glow discharge particles along the quadrupole axis by means of a thin metal capillary. The ionization of sample molecules occurs inside the RF quadrupole, which is also the first stage of the OA–TOF–MS interface. The pressure of the buffer gas inside the quadrupole is 20–150 Pa and depends on the flow rates of the gas flow from the discharge zone and the gas sample. The ions transferred by the gas-dynamic interface get into the high-resolution OA–TOF–MS.

As test gas samples (**TGSs**), a helium–octane mixture with a molar concentration of *n*-octane of 100 ppb (test gas TGS-1) and a helium–toluene mixture with a molar concentration of toluene of 100 ppb (TGS-2). The mixtures were prepared in a 192-L stainless steel tank. A vacuum was created in the tank; then a calculated amount of either *n*-octane (1.4 μL) or toluene (0.9 μL) was injected with simultaneous helium flow into the tank. The resulting mixture was then diluted with helium with 1 : 10 ratio. To create a glow discharge, two electrodes were placed outside the glass tube at a distance of 50 mm from its output end and at a distance of 2–3 cm from each other. The amplitude of the RF voltage at the quadrupole was varied in the range 0–90 V, and the frequency was 1.4 MHz. A flat diaphragm 0.1 mm in thickness with an aperture of 0.5 mm in diameter was placed behind the quadrupole. Behind the diaphragm, there was the large segmented RF quadrupole with 8 mm rod diameter and 17 cm rod length, where sample ions entering the aperture of the diaphragm were focused. The pressure in this quadrupole was 0.5–1.5 Pa and depended on the gas flow rate into the discharge zone.

RESULTS AND DISCUSSION

In case of argon as a discharge gas, the background mass spectrum (in the absence of TGS) contains four main intensive peaks corresponding to Ar^+, ArH^+, Ar_2^+ and Ar_2H^+ ions. These ions could be formed in a glow discharge and transported to the quadrupole with the argon flow. They can also arise as a result of ion-molecular reactions [28, 29]. There are also minor peaks of H_2O, O_2, and N_2 impurities in the background mass spectrum. We note that the excitation energies of metastable Ar* argon atoms are insufficient to ionize H_2O or N_2 (Table 1). The cross sections for the Penning ionization of O_2 in the collision with Ar* atoms at the thermal energy are 1.2×10^{-16} ($Ar^*4^3P_0$) and 1.8×10^{-16} cm^2 ($Ar^*_{43}P_2$) [30]; therefore, we can expect the formation of $O_2^{+\bullet}$ ions as a result of the interaction of Ar* with O_2 molecules.

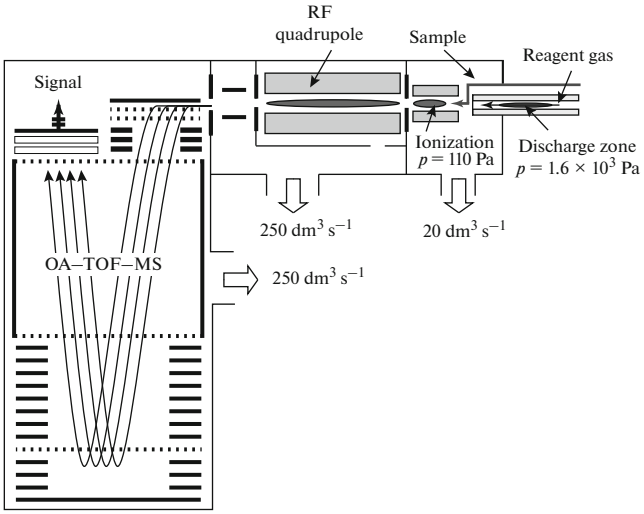

Fig. 1. Block diagram of the experimental setup consisting of OA–TOF–MS and the ion source. Resolution of the instrument, $R \approx 10000$ (FWHM); accuracy of determination of m/z, of the order of 10 ppm; the electrodeless low-pressure capacitive glow discharge with p = 150–2500 Pa, U = 500 V (p–p), ν = 400–800 kHz.

It was interesting to evaluate the efficiency of *n*-octane detection in this ion source, because even in the case of "soft" ionization, *n*-octane gives intense peaks of fragments and is more difficult to identify than aromatic compounds. We obtained mass spectra using the proposed ion source with argon discharge for TGS-1 (*n*-C_8H_{18} (*n*-octane) in He, the *n*-C_8H_{18} concentration is 100 ppb) with turned on and turned off RF voltage on the quadrupole of the ion source (Figs. 2a and 2b); for comparison, the mass spectrum of *n*-octane from the NIST library obtained under electron ionization conditions (70 eV) is given (Fig. 2c). The composition of the peaks in all three spectra coincides; however, the intensity of the peak of *n*-octane molecular ion $C_8H_{18}^{+\bullet}$ in the spectra obtained in the ion source with a glow discharge (15% of the total intensity of molecular ion and fragment ions) is much higher (more than tenfold) than in the spectrum of electron ionization.

Figure 3 shows the dependences of the ion peak intensities in the mass spectra of TGS-1 on the argon flux from the discharge zone. The peaks of the sample ions appear in the mass spectrum at the argon flow rate of approximately 250 cm^3 min^{-1}. Dependences for the molecular ion $C_8H_{18}^{+\bullet}$ and for the sum of the sample ions are similar and show maximal intensity for the argon flow of 500 cm^3 min^{-1}. When the amplitude of the RF voltage at the quadrupole of the ion source increases from 0 to 46 V, the intensity of the peak of $C_8H_{18}^{+\bullet}$ decreases by approximately threefold, and the

Table 1. Metastable states of atoms and ionization energies of atoms and molecules

Atom, molecule	Metastable state	Excitation energy, eV	Life time, s	Ionization energy, eV
He	2^3S_1	19.82	8000	24.59
	2^3S_0	20.62	0.02	
Ar	4^3P_0	11.72	45	15.76
	4^3P_2	11.55	56	
O_2				12.07
N_2				15.58
H_2O				12.61
$C_6H_5CH_3$				8.82
n-C_8H_{18}				10.03

total intensity of the peaks of the sample ions increases by ~25%. The fall in the intensity of the molecular ion peak can be explained by the activation of ion-molecular reactions that lead to molecular ion decay as a result of an increase in the collision energy of an ion with gas molecules. The increase in the total intensity of sample ions is associated with more efficient transport of ions to the next stage of the mass spectrometer interface due to the focusing in the RF quadrupole.

Note that the ionization region is located inside the RF quadrupole. The mean free path of $C_8H_{18}^{+\bullet}$ ions in argon at a pressure of 50 Pa is ~0.5 mm, and the inscribed diameter of the quadrupole is 5 mm. Consequently, moving between two sequential collisions with argon atoms, ion $C_8H_{18}^{+\bullet}$ can gain an energy of ~10% of the voltage between the quadrupole rods, which is twice the amplitude of the RF voltage, that is, ~90/10 = 9 V. In the collision with an argon atom, the energy is ~$(M_{Ar}/M_{C_8H_{18}}) \times 9$ V = 3.2 V. This energy can be sufficient for the fragmentation of the $C_8H_{18}^{+\bullet}$ ion. Note that the effect of collision fragmentation of ions upon focusing by the radio-frequency field is weakened with increasing ion mass and decreasing the ratio of argon and sample ions. On the other hand, free electrons can be carried out with the argon flux from the discharge zone to the ionization region. The mean free path of an electron is close to the mean free path of a molecular ion, that is, ~0.5 mm. The average electron energy between collisions is ~9 eV, but near the rods, the electric field strength is 2.5–3 times higher; therefore, electrons with an energy of ~25 eV, sufficient for electron ionization of an n-octane molecule, can appear. Fragmentation accompanying the electron ionization can lead to an increase in the intensity of fragment ions in the mass spectrum as well (Fig. 2b).

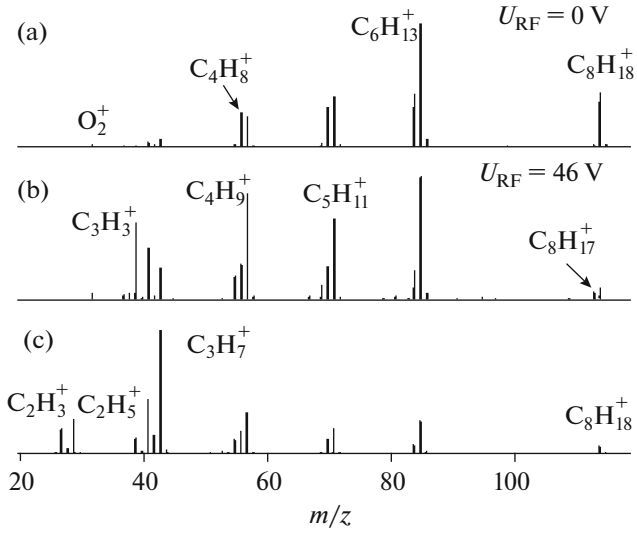

Fig. 2. (a and b) Mass spectra of n-octane obtained at different amplitudes of the RF voltage on the quadrupole locatedin the ionization region (the recording time, 10 s; the rate of the argon flow from the discharge zone, 500 cm^3 min^{-1}; the flow rate of TGS-1, 10 cm^3 min^{-1}) and (c) electron ionization mass spectrum of n-octane from the NIST spectral library.

Another way of the appearance of fragment ions can be the ion-molecular reaction of the $C_8H_{18}^{+\bullet}$ ion with the C_8H_{18} molecule. For example, a decrease in the intensity of $C_8H_{18}^{+\bullet}$ ions and an increase in the intensity of $C_8H_{17}^+$ ions were observed with an increase in the concentration of n-octane molecules in the ion source [31].

The flow of sample molecules to the ionization region is ~4×10^{11} molecules s^{-1}; the flow of detectable ions in the mass spectra is 3.3×10^2 ion s^{-1} for molecular n-octane ions and 3.0×10^3 ion s^{-1} for the sum of all sample ions. The measured efficiency of n-octane detection with respect to the total ion current is ~10^{-8} ions per molecule. The detection efficiency of

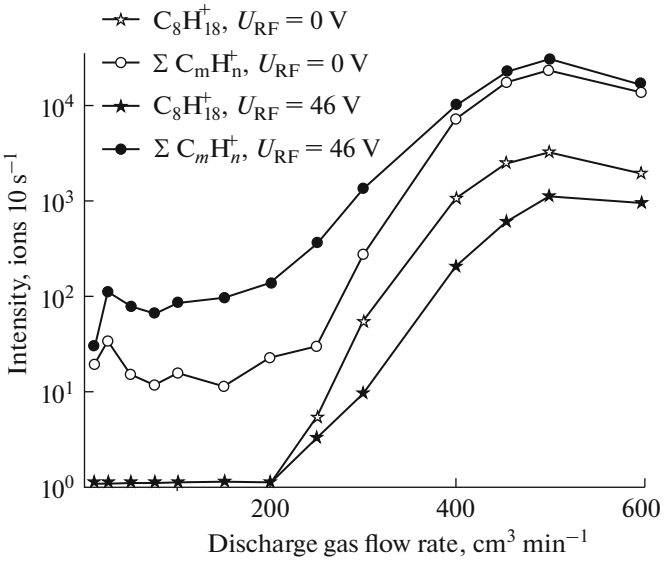

Fig. 3. Dependencies of the ion intensities in the mass spectra of TGS-1 on the argon flow rate (the flow rate of TGS-1, 10 cm^3 min^{-1}). The data are presented for the cases of the switched off and switched on RF voltage at the ion source quadrupole.

the molecular ion of *n*-octane is ~10^{-9} ions per molecule, or 5 ions pg^{-1}.

In the ion source presented, the function of a glow discharge consists in the formation of excited Ar* atoms. As noted above, the Ar* concentration in the glow discharge zone is ~10^9 to 10^{11} cm^{-3} in the pressure range of 100–10^5 Pa [18, 19]; based on the published data, it is difficult to expect a higher concentration of Ar* in a glow discharge. For effective ionization of the analyte, it is important to transport Ar* atoms from the discharge zone to the ionization region, which is several centimeters downstream of the gas flow, with as little loss as possible. To estimate the concentration of Ar* atoms in the ionization region, the flow of argon in the discharge tube and in the RF quadrupole was simulated using the ANSYS 14.0 software. Gas-dynamic simulation yielded two-dimensional arrays of the velocities, densities, pressures, and temperatures of argon in this system (Figs. 4 and 5).

Since the density of argon decreases in the direction of the flow toward the ionization region, the concentration of Ar* atoms decreases. We note that this

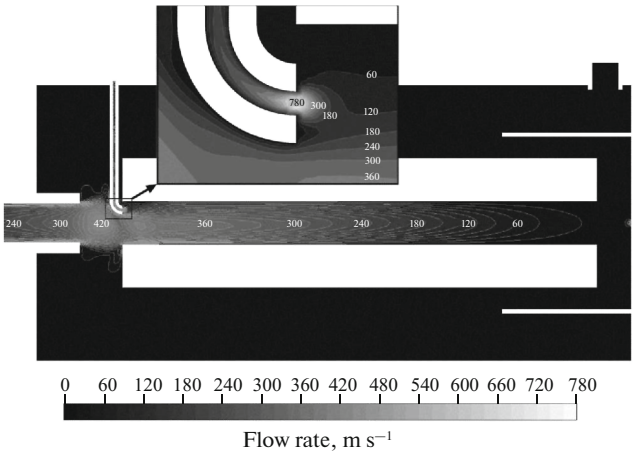

Fig. 4. Profile of the gas velocity in the RF quadrupole at an argon flow rate through the tube of 500 cm^3 min^{-1} and a TGS flow rate of 10 cm^3 min^{-1}.

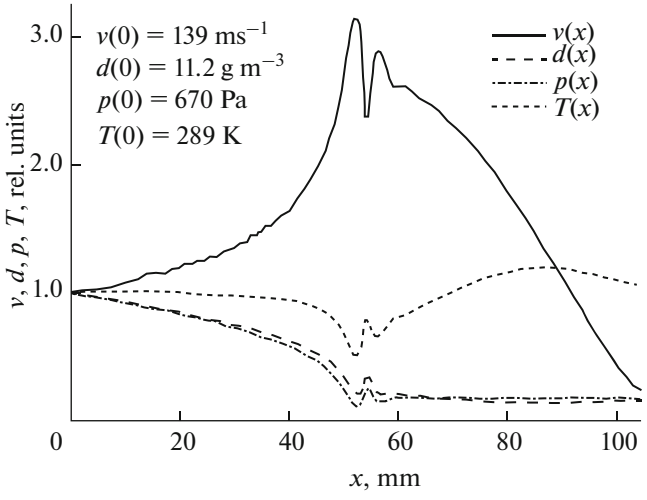

Fig. 5. Velocity, density, pressure, and temperature of the gas on the axis of the system consisting of a tube (internal diameter, 4.5 mm, and length, 50 mm) and an RF quadrupole; the flow rate of argon through the discharge tube, 500 cm^3 min^{-1}; the flow rate of TGS is 10 cm^3 min^{-1}.

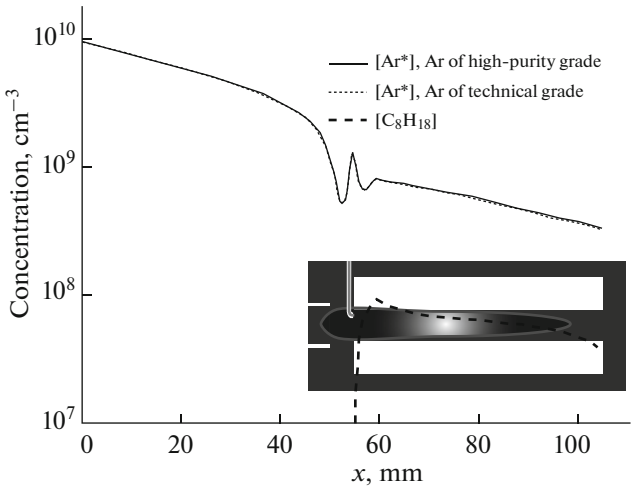

Fig. 6. Dependencies of Ar* atoms and sample molecules concentration on the axis of the system (discharge tube–RF quadrupole) for two types of argon (high purity and technical grades); the flow rate of argon through the discharge tube, 500 cm^3 min^{-1}; the flow rate of sample, 10 cm^3 min^{-1}

effect is the higher, the higher the degree of expansion of argon from the discharge tube to the ionization chamber; thus, it is disadvantageous to supply argon to the ionization region along a thin tube. An additional contribution to the drop in the concentration of Ar* atoms is made by quenching of Ar* atoms excitation in collisions with Ar atoms (homogeneous reaction (1)) and with the inner surface of the glass tube (heterogeneous reaction (2)):

$$Ar^* + Ar \rightarrow Ar + Ar + h\nu\ (k_C)\ (1),$$

$$Ar^* + Wall \rightarrow Ar\ (k_W)\ (2).$$

The change in the concentration of Ar* atoms in the gas flow can be written as

$$\nabla(v(x)[Ar^*](x)) = -(k_C[Ar](x) + k_W)[Ar^*](x), \quad (1)$$

where k_C is the homogeneous collision quenching constant, k_W is the heterogeneous quenching constant, $v(x)$ is the gas flow rate in the tube, [Ar*] is the concentration of metastable atoms, and [Ar] is the concentration of gas atoms.

Expressions for the rate constants k_C and k_W are

$$k_C = \sigma_E V_{Ar}, \quad (2)$$

$$\frac{1}{k_W} = \frac{1}{k_W^{kin}} + \frac{1}{k_W^{diff}}, \quad k_W^{kin} = \frac{\gamma V_{Ar}}{2R}, \quad k_W^{diff} = 5.78\frac{D_{Ar^*}}{R^2}, \quad (3)$$

where σ_E is the quenching cross section of Ar* atoms by Ar atoms, V_{Ar} is the average thermal velocity of Ar atoms, γ is the probability of quenching of Ar* atoms at the surface of the tube, R is the tube radius, and D_{Ar^*} is the diffusion coefficient of Ar* atoms in argon [32–35].

The value of k_W^{kin} (in the case of $0.5 < \gamma < 0.85$ [36]) is an order of magnitude larger than the value of k_W^{diff} even in the region of the gas flow with the lowest pressure (ionization region). Thus, $k_W \approx k_W^{diff}$.

This estimate does not take into account the homogeneous quenching of Ar* atoms in collisions with electrons. The rate constant of such a process is rather large, but it is difficult to estimate the concentration of electrons in a gas moving from the discharge zone.

Using Eq. (1), an expression was obtained for the relative change in the concentration of Ar* atoms in the discharge tube and the RF quadrupole as a function of distance x from the glow discharge zone, that is,

$$\frac{\alpha(x)}{\alpha(x=0)} = \theta(x)\exp\left(-\beta\int_0^x \theta^2(x)dx - \delta\int \frac{p_{rel}^2(x)}{\theta(x)}dx\right), \quad (4)$$

where $\alpha(x) = \frac{[Ar^*](x)}{[Ar](x)}$, $\theta(x) = \frac{T(x)}{T_0}$, $\beta = \frac{5.78\pi k_B n_{Ar} D_{Ar^*} T^0}{Q}\theta^2(x)$, $\delta = \frac{n_L(T_0)\pi R^2 k_C p_q^2}{Q}$, $p_{rel}(x) = \frac{p(x)}{p_q}$, $T_0 = 295$ K, $p_q = 106$ Pa (pressure in the ionization region at the argon flow rate in the discharge tube of $Q = 500$ cm^3 min^{-1}), and R is the inner radius of the tube.

The values of the diffusion coefficient and the quenching cross section of Ar* atoms in argon at 300 K are taken from publications: $n_{Ar}D_{Ar^*} = 1.9 \times 10^{18}$ cm^{-1} s^{-1} [37], $\sigma_E = 2 \times 10^{-20}$ cm^2 for Ar* (4^3P_2) and 10^{-19} cm^2 for Ar* (4^3P_0) [38]; the latter value was used in the calculations. Using the distributions of the velocity, pressure, and temperature of argon in the tube and in the RF quadrupole, obtained by gas-dynamic simulation (Fig. 5), the dependencies of the concentration of Ar* atoms and sample molecules in this system were determined (Fig. 6). In addition, the calculations took into account the quenching processes of Ar* atoms at impurity molecules in argon (N_2, H_2O, CO_2, and O_2), as their allowance differs for different grades of argon. For technical grade argon these values are 0.01, 0.001, 0.001 and 0.002% respectively.

To estimate the ionization efficiency of *n*-octane molecules by Ar* atoms, it is necessary to know the Penning ionization cross section of the process. We found the cross sections for Penning ionization by Ar* (4^3P_2) atoms of Zn and Cd atoms in the literature, which make up 5.3×10^{-15} and 6.5×10^{-15} cm^2 for

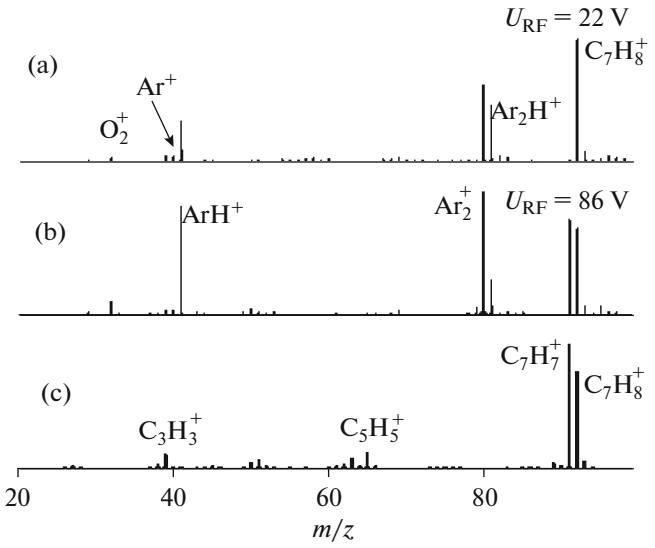

Fig. 7. (a and b) Mass spectra of toluene obtained at different amplitudes of the RF voltage on the quadrupole in the ionization region (the rate of the argon flow from the discharge zone, 500 cm^3 min^{-1}; the flow rate of TGS-2, 10 cm^3 min^{-1}; the recording time, 10 s) and (c) electron ionization mass spectrum of toluene from the NIST spectral library.

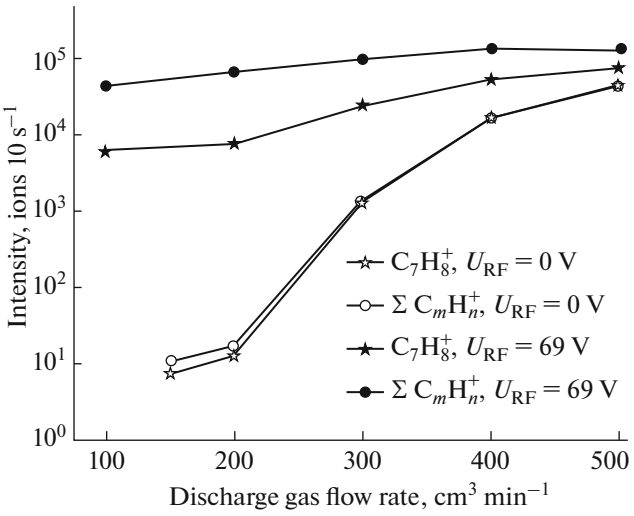

Fig. 8. Dependences of the ion intensities in the mass spectra of TGS-2 on the argon flow rate (the flow rate of TGS-2, 10 cm^3 min^{-1}). The data are presented for the cases of the switched off and switched on RF voltage on the quadrupole of the ion source.

thermal collision energies [30]; the latter value was used for calculations.

Assuming that the Penning ionization cross sections for alkanes are close in order of magnitude to the collision cross sections of these molecules with Ar* atoms, the collision frequency of *n*-octane molecules with Ar* is

$$\nu = n_{Ar^*} V_{Ar} \sigma_{PI}, \quad (5)$$

where n_{Ar^*} is the concentration of Ar* atoms in the ionization region, and σ_{PI} is the Penning ionization cross section. The average thermal velocity of Ar atoms (V_{Ar}) at a temperature of 300 K is 4×10^4 cm s^{-1}.

Assuming the dependence of the concentration of Ar* atoms and *n*-octane molecules in the ionization region stationary (Fig. 6) and taking the inscribed volume of the quadrupole as the volume of the reactor, the value of the number of *n*-octane ions formed in such a reactor in 1 s was obtained (~7×10^6 ions). Consequently, an evaluation of the efficiency of the Penning ionization of *n*-octane yields a value of ~2×10^{-5} ions per molecule. Note that the experimental efficiency of detecting *n*-octane using the described ion source was ~10^{-8} ions per molecule.

The efficiency of sample detection also depends on the ion transport efficiency from ionization region to mass analyzer and the registration efficiency of these ions by a mass analyzer. Based on the experimental data obtained earlier for ions with *m/z* 50–100 at the OA–TOF–MS used in this work, we estimate the maximal transport efficiency of molecular ions of *n*-octane and their fragments from the quadrupole to the mass analyzer as ~10^{-2} The detection efficiency for *m/z* 50–100 by means of an orthogonal-acceleration time-of-flight mass spectrometer is ~10^{-1}, so we assume the total loss factor to be ~10^{-3}.

Many researchers [16, 17, 39] report the sensitivity in the analysis of aromatic compounds to demonstrate the characteristics of mass spectrometric systems. To compare the characteristics of our source with other systems, experiments were performed with a sample of toluene in helium. Below are the results of measurements for a sample of TGS-2 ($C_6H_5CH_3$ in helium, the concentration of $C_6H_5CH_3$ is 100 ppb) (Fig. 7). The intensity of the obtained peak of the toluene molecular ion $C_7H_8^{+\bullet}$ is 96% of the total intensity of the molecular ion and fragment ions, while in the electron ionization mass spectrum, this value is 29%.

The dependencies of toluene molecular ion intensity and the total sample ions intensity on the argon flow (Fig. 8) demonstrate additional capabilities of using the RF quadrupole in the ion source.

The radio-frequency field increases the detection efficiency of the sample and makes it possible to work with smaller discharge gas flows. However, the fraction of the molecular ion in the total intensity of the sample ions decreases.

In the mass spectra of toluene (Fig. 7), there are signals of Ar^+, ArH^+, Ar_2^+, and Ar_2H^+ ions; however, the significant participation of these ions in the ionization of toluene molecules is not confirmed experimentally (Fig. 9).

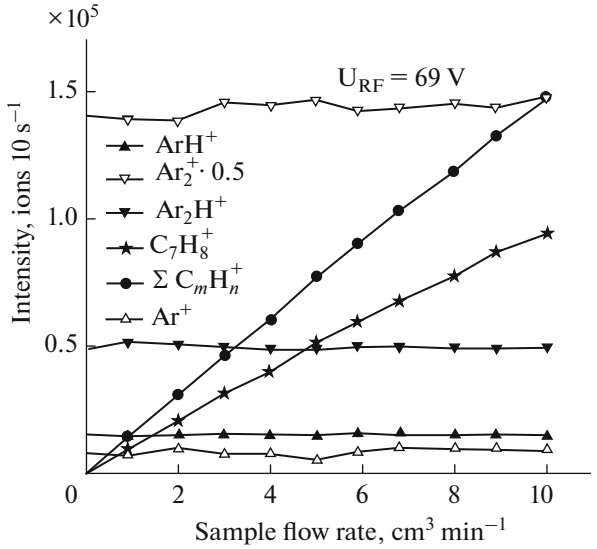

Fig. 9. Dependences of the ion intensities in the mass spectra of TGS-2 on the argon flow rate (the flow rate of argon from the discharge zone, 500 cm^3 min^{-1}).

The intensity of the peak of molecular ions of toluene $C_7H_8^{+\bullet}$ in the mass spectrum increases linearly with increasing sample flow; the change in the intensity of toluene ions is at least an order of magnitude greater than the variation in the intensities of ions containing argon atoms. The on-line method for sample injection used in this study enabled the verification of the linear correspondence of the signal to the sample flux only in the range of one order of magnitude. The flux of toluene molecules during the sample injection in helium was 4×10^{11} molecules s^{-1} or 60 pg s^{-1}. Approximately 8×10^3 molecular ions of toluene were recorded per second and $\sim 1.5 \times 10^4$ of all toluene ions per second. Consequently, the experimental detection efficiency of toluene is $1.5 \times 10^4/4 \times 10^{11} \approx 4 \times 10^{-8}$ ions per molecule. The magnitude of the chemical noise was in this case in the range of 0–5 ions s^{-1}.

Taking into account the loss factor in the transport and detection of ions in OA–TOF–MS ($\sim 10^{-3}$), this value is in good agreement with the estimation of the maximum ionization efficiency ($\sim 2 \times 10^{-5}$ ions per molecule).

The difference in the detection efficiency of *n*-octane and toluene is probably associated with the use of a radio-frequency quadrupole for transporting ions from the ion source to the mass analyzer. With Penning ionization of *n*-octane, as well as in electron ionization (Fig. 2c), light fragment ions can be formed, for example, CH_3^+, $C_2H_3^+$, $C_2H_5^+$; the transport efficiency of such ions is lower because of instability of light ions motion in RF quadrupole.

Thus, the detection efficiency of toluene molecular ions in our work is $\sim 2 \times 10^{-8}$ ions per molecule or ~130 ions pg^{-1}. In [16], the sensitivity is 800 rel. units pg^{-1}. It is difficult to recalculate accurately this quantity into ions per picogram (ions pg^{-1}). However, if we assume that in absence of ions the noise signal is usually 5 rel. units s^{-1}, then the signal of 800 rel. units pg^{-1} corresponds to ~160 ions pg^{-1}. Thus, the value obtained in this work is close to the sensitivity given in [16], at least twice exceeds the sensitivity given in [17] (60 counts pg^{-1}), and by more than three orders of magnitude higher than that in the SIFT method (1 ion per 10 ppbv for the flow of 60 cm^3 min^{-1}, which corresponds to the efficiency of 4×10^{-12} ions per molecule or 0.04 ions pg^{-1}) [39].

CONCLUSIONS

The minimal detectable concentrations of *n*-octane and toluene samples in helium were estimated for a signal-to-noise ratio of 3. Using the described experimental configuration of an ion source, the limits of detection for 1 s are as follows: $(10^{-7}/330) \times 10 \approx 3.0 \times 10^{-9}$ (3 ppb or 2.3 pg) for molecular *n*-octane ions and $(10^{-7}/8000) \times 10 \approx 1.3 \times 10^{-10}$ (0.13 ppb or 0.08 pg) for molecular toluene ions.

The used version of a glow discharge is simple and cheap, consumes little power, and is free of contamination on metal electrodes resulting in contact with the discharge.

The ion source with Penning ionization, proposed in our work, can be easily constructed from an atmospheric pressure ionization ion source by substitution of one interface element (heated capillary) for a quartz tube with a glow discharge.

Radio-frequency devices (quadrupole or ion funnel) are conventional elements of mass spectrometric interfaces with atmospheric pressure ionization. The use of a radio-frequency quadrupole in the Penning ionization region can be useful in analyzing aromatic compounds and organic molecules with mass considerably exceeding that of the discharge gas atoms.

We expect that a combination of such an ion source with OA–TOF–MS can be used to control and identify impurities of various organic compounds in a gas sample in real time, which is very important, in particular, for solving ecological problems in analytical chemistry.

REFERENCES

1. Beynon, J.H., *Mass Spectrometry and Its Application to Organic Chemistry*, Amsterdam: Elsevier, 1960.
2. Amirav, A., Gordin, A., Poliak, M., et al., *J. Mass Spectrom.*, 2008, vol. 43, no. 2, p. 141.
3. Talroze, V.L. and Lyubimova, A.K., *Dokl. Akad. Nauk SSSR*, 1952, vol. 86, no. 4, p. 909.

4. Munson, M.S.B. and Field, F.H., *J. Am. Chem. Soc.*, 1966, vol. 88, no. 12, p. 2621.
5. Kebarle, P., *J. Am. Soc. Mass Spectrom.*, 1992, vol. 3, no. 1, p. 1.
6. Lipsky, S.R. and Shanin, M.M., *Nature*, 1963, vol. 197, no. 4867, p. 625.
7. Anderson, D.R., Bierbaum, V.R., Depuy, C.H., et al., *Int. J. Mass Spectrom. Ion Phys.*, 1983, vol. 52, no. 1, p. 65.
8. McLuckey, S.A., Glish, G.L., Asano, K.G., et al., *Anal. Chem.*, 1988, vol. 60, no. 20, p. 2220.
9. Andrade, F.J., Shelley, J.T., Wetzel, W.C., et al., *Anal. Chem.*, 2008, vol. 80, no. 8, p. 2646.
10. Boutin, M., Lesage, J., Ostiguy, C., et al., *J. Am. Soc. Mass Spectrom.*, 2004, vol. 15, no. 9, p. 1315.
11. Ganeev, A.A., Gubal, A.R., Uskov, K.N., et al., *Russ. Chem. Bull.*, 2012, vol. 61, no. 4, p. 752.
12. Faubert, D., Paul, G.J.C., Giroux, J., et al., *Int. J. Mass Spectrom. Ion Processes*, 1993, vol. 124, no. 1, p. 69.
13. Hiraoka, K., Fujimaki, S., Kambara, S., et al., *Rapid Commun. Mass Spectrom.*, 2004, vol. 18, no. 19, p. 2323.
14. Ganeev, A.A., Kuzmenkov, M.A., Potapov, S.V., et al., RF Patent 2251686, 2005.
15. Verenchikov, A. and Zamyatin, A., US Patent 9070541, 2012.
16. Verenchikov A.N. and Kolosov A.P., *Mass-Spektrom.*, 2014, vol. 11, no. 4, p. 206.
17. Jordan, A., Haidacher, S., Hanel, G., et al., Int. *J. Mass Spectrom. Ion Processes*, 2009, vol. 286, no. 1, p. 32.
18. Bogaerts, A., Guenard, R.D., Smith, B.W., et al., *Spectrochim. Acta, Part A*, 1997, vol. 52, no. 2, p. 219.
19. Garcia, M.C., Rodero, A., Sola, A., et al., *Spectrochim. Acta, Part A*, 2000, vol. 55, no. 11, p. 1733.
20. Kozlovskii, V.I., Sulimenkov, I.V., Brusov, V.S., et al., RF Patent 2529009, 2014.
21. Sulimenkov, I.V., Brusov, V.S., Pikhtelev, A.R., et al., in *Proc. 5th Int. Conf.-School "Fundamental Issues of Mass Spectrometry and Its Analytical Application,"* St. Petersburg, 2013, p. 64
22. Sulimenkov, I.V., Brusov, V.S., Pikhtelev, A.R., et al., in *Mater. 5th Mezhdunar. Conf. "Mass-spektrometria i ee prikladnye problemy"* (*Proc. 5th Int. Conf. on Mass Spectrometry and Problems of Its Applications*), Moscow, 2013, p. 119.
23. Sulimenkov, I.V., Brusov, V.S., in *Mater. 6th Mezhdunar. Conf. "Mass-spektrometria i ee prikladnye problemy"* (*Proc. 6th Int. Conf. on Mass Spectrometry and Problems of Its Applications*), Moscow, 2015, p. 113.
24. Dodonov, A.F., Kozlovski, V.I., Soulimenkov, I.V., et al., *Eur. J. Mass Spectrom.*, 2000, vol. 6, no. 6, p. 481.
25. Dodonov, A., Kozlovsky, V., Loboda, A., et al., *Rapid Commun. Mass Spectrom.*, 1997, vol. 11, no. 15, p. 1649.
26. Dodonov, A., Kozlovski, V., Sulimenkov, I., et al., *Proc. 47th ASMS Conf. on Mass Spectrometry and Allied Topics*, Dallas, TX, 1999.
27. Sulimenkov, I.V. and Kozlovskii, V.I., Pikhtelev, A.R., et al., *Mass-Spektrom.*, 2005, vol. 2, no. 3, p. 217.
28. Lindinger, W., *Phys. Rev. A: At., Mol., Opt. Phys.*, 1973, vol. 7, no. 1, p. 328.
29. Carazzato, D. and Bertrand, M.J., *J. Am. Soc. Mass Spectrom.*, 1994, vol. 5, no. 4, p. 305.
30. *Fizicheskie velichiny. Spravochnik* (Physical Quantities: Reference Book), Grigorev, I.S. and Meilikhov, E.Z., Moscow: Energoatomizdat, 1991.
31. Hiraoka, K., Furuya, H., Kambara, S., et al., *Rapid Commun. Mass Spectrom.*, 2006, vol. 20, no. 21, p. 3213.
32. Smirnov, B.M., *Phys.-Usp.*, 1981, vol. 24, no. 4, p. 251.
33. Smirnov, B.M., *Iony i vozbuzhdennye atomy v plazme* (Ions and Excited Atoms in a Plasma), Moscow: Atomizdat, 1974.
34. Frank-Kamenetskii, D.A., in *Diffuziya i teploperedacha v khimicheskoi kinetike* (Diffusion and Heat Transfer in Chemical Kinetics), Moscow: Nauka, 1987, p. 71.
35. Gershenzon, Yu.M., Grigorieva, V.M., Ivanov, A.V., et al., *Faraday Discuss.*,1995, vol. 100, p. 83.
36. Smirnov, B.M., in *Vozbuzhdennye atomy* (Excited Atoms), Moscow: Energoizdat, 1982, p. 46.
37. Smirnov, B.M., in *Vozbuzhdennye atomy* (Excited Atoms), Moscow: Energoizdat, 1982, p. 33.
38. Smirnov, B.M., in *Vozbuzhdennye atomy* (Excited Atoms), Moscow: Energoizdat, 1982, p. 62.
39. Spanel, P. and Smith, D., *Med. Biol. Eng. Comput.*, 1996, vol. 34, no. 6, p. 409.

Translated by O. Zhukova